

Quantum Filter Diagonalization: Quantum Eigendecomposition without Full Quantum Phase Estimation

Robert M. Parrish^{1,*} and Peter L. McMahon^{1,2}

¹ *QC Ware Corporation, Palo Alto, CA 94301*

² *School of Applied Engineering and Physics, Cornell University, Ithaca, NY 14853*

We develop a quantum filter diagonalization method (QFD) that lies somewhere between the variational quantum eigensolver (VQE) and the phase estimation algorithm (PEA) in terms of required quantum circuit resources and conceptual simplicity. QFD uses a set of time-propagated guess states as a variational basis for approximate diagonalization of a sparse Pauli Hamiltonian. The variational coefficients of the basis functions are determined by the Rayleigh-Ritz procedure by classically solving a generalized eigenvalue problem in the space of time-propagated guess states. The matrix elements of the subspace Hamiltonian and subspace metric matrix are each determined in quantum circuits by a one-ancilla extended swap test, i.e., statistical convergence of a one-ancilla PEA circuit. These matrix elements can be determined by many parallel quantum circuit evaluations, and the final Ritz estimates for the eigenvectors can conceptually be prepared as a linear combination over separate quantum state preparation circuits. The QFD method naturally provides for the computation of ground-state, excited-state, and transition expectation values. We numerically demonstrate the potential of the method by classical simulations of the QFD algorithm for an $N = 8$ octamer of BChl-a chromophores represented by an 8-qubit *ab initio* exciton model (AIEM) Hamiltonian. Using only a handful of time-displacement points and a coarse, variational Trotter expansion of the time propagation operators, the QFD method recovers an accurate prediction of the absorption spectrum.

I. INTRODUCTION

The effective extraction of a few low-lying eigenpairs and corresponding transition operator expectation values from a large Hermitian matrix specified in sparse Pauli form is a ubiquitous task in mathematical physics and optimization. In the former consideration, the operator to be diagonalized is often a representation of the Hamiltonian for an interesting quantum system, and the diagonalization amounts to solving the time-independent Schrödinger equation within this representation. In the latter consideration, the operator to be diagonalized is a classical Ising Hamiltonian that is isomorphic to the cost matrix of a binary optimization problem. Here, the matrix is already diagonal in the \hat{Z} basis, and the eigendecomposition amounts to an exhaustive search for low-lying diagonal matrix elements.

Numerous classical approaches have been developed to approximately solve this problem, but all require extensive validation efforts to ensure sufficient accuracy for each new class of physical problem encountered. In particular, most such approximations rely on perceived spatial-, rank-, or tensor-sparsity structure in the physical problems at hand, in an attempt to ameliorate the exponential naive classical cost of representing even a single eigenpair directly. E.g., in the diagonalization of quantum Hamiltonians of electronic structure theory, a myriad of approximate theories ranging from density functional theory,¹⁻⁴ coupled cluster theory,⁵⁻¹⁰ selected configuration interaction theory,¹¹⁻¹⁷ and density matrix renormalization group theory^{18,19} has been developed - each performs remarkably well in certain regimes of the problem space, and fails qualitatively in others. A promising alternative approach is to use a univer-

sal quantum computer to aid in part of the computation. As increasingly powerful quantum circuit hardware becomes available, this approach will remove formal tractability barriers regarding the storage and manipulation of Hilbert space quantities, but will surely be fraught with conceptual challenges involving the design of efficient hybrid quantum/classical algorithms that will have only limited few-qubit quantum circuit gates and that will necessarily output only quantum observable measurements. Numerous impressive strides have been made over the past few decades in developing efficient algorithms along these lines. A foundational algorithm for quantum eigendecomposition is the phase estimation algorithm (PEA).²⁰⁻²⁷ Unfortunately, phase estimation requires nested control of Trotterized time propagation operations by a large array of ancilla qubits, which, when expanded to the standard library of 1- and 2-qubit gates, yields extremely long circuits which will not be tractable in the near term. Motivated by the limited gate depths and low fidelity of extant noisy intermediate-scale quantum (NISQ) devices,²⁸ several compelling “variational quantum algorithms” have been developed over the past few years that feature vastly lowered gate requirements (and usually no ancilla qubits) at the cost of designing and optimizing a heuristic variational entangler circuit. An archetypical method of this type is the variational quantum eigensolver (VQE),²⁹ which has been widely deployed in simulators and in several types of quantum hardware to target the lowest eigenstates of the Hamiltonian for electrons in molecules and other physical systems.²⁹⁻³⁶ VQE has seen numerous recent extensions to efficiently treat excited states,^{29,37-42} transition properties,⁴² and gradient properties.⁴³⁻⁴⁵ A doppelgänger of VQE in the area

of optimization is the quantum approximate optimization algorithm (QAOA),⁴⁶ which also uses a specially constructed variational entangler circuit to attempt to approximate diagonalization of a classical Ising Hamiltonian. A large body of work has been devoted to the practical utilization of QAOA and variants to provide direct optimization of practically-relevant binary optimization problems.^{47–57} VQE and QAOA often produce accurate results with short quantum circuits relative to more-traditional quantum algorithms, but the *ad hoc* definitions of the variational entangler circuits remain a significant barrier to analysis and routine black-box deployment of these methods. Moreover, the difficult nonlinear optimization procedure of the variational circuit parameters has proven to be a difficult practical aspect of variational quantum algorithms, with such conceptual nightmares encountered as “barren plateaus” of vast regions of the parameter space that are far from optimal and have vanishing gradient information.⁵⁸

In the present work, we develop an algorithm we refer to as “quantum filter diagonalization” (QFD) that conceptually lives somewhere between VQE and PEA. The algorithm starts from a set of easily classically prepared approximate reference states for the targeted eigenvectors, and then builds a variational ansatz of a linear combination of time-advanced and time-delayed reference states. The preparation of time-advanced and time-delayed reference states are conceptually prepared by application of the Trotterized time propagation operator on quantum circuit hardware. Key to the algorithm is the evaluation of both Hamiltonian and metric transition expectation values over different pairs of time-advanced and time-delayed reference states: a single-ancilla variant of the quantum swap test is found to be sufficient for this purpose. Finally, the algorithm concludes with a classical diagonalization of the generalized eigenvalue problem involving the quantum Hamiltonian and metric matrix elements evaluated over time-advanced and time-delayed reference states. The resultant classical eigenvalues are variational estimates of the eigenvalues of the full Hamiltonian, while the classical eigenvectors provide a recipe for the classical mixing of time-advanced and time-delayed reference states to reconstruct the approximate eigenvectors in the full space. Post-facto evaluation of matrix elements in the quantum circuit hardware then enables the extraction of transition property expectation values over other sparse Pauli-basis Hermitian operators.

The use of a grid of time-propagated states as a basis for quantum eigendecomposition algorithms is certainly not new - in fact, it can be argued that the original phase estimation algorithm was founded on just such a basis. Some time ago, Somma *et al* proposed an algorithm⁵⁹ based on taking the discrete Fourier transform of observables evaluated over a regularly-spaced time propagation grid, but this method only works well when there are a small number of distinct and well-separated eigenvalues. More recently, O’Brien *et al* published an interesting time-grid method⁶⁰ based on a Prony-type fitting

of the relative time-shift overlap matrix. Kyriienko has also published a highly compelling “quantum inverse iteration” method⁶¹ that uses a time propagation grid with a predetermined quadrature recipe to approximate the operator $(\hat{H} - \lambda)^{-\alpha}$ where λ is a guess for the target eigenvalue and $\alpha \geq 1$. When this operator is applied to a guess eigenstate, the component of the eigenvector nearest to λ is significantly magnified, improving the solution. Very recently, as we were finalizing the numerical demonstrations for this manuscript, Somma published yet another interesting time grid method⁶² that uses a Fourier series for a smooth cutoff function to extinguish high-lying eigenvectors. The novelty of our approach is primarily in the explicit use of the time-propagated states as a variational basis ansatz for the full eigenstates. This necessitates the evaluation of the variational basis subspace Hamiltonian and metric matrices (evaluated in the proposed method with quantum circuits by using an extension of the swap test) followed by a classical generalized eigensolution. We also point out that our “quantum filter diagonalization” approach is heavily inspired by the classical filter diagonalization approach,^{63–68} which uses a basis of either time-propagated reference states or a Chebyshev expansion of $(\hat{H} - \lambda)^{-\alpha}$ acting on reference states. The first of these variants closely resembles the flavor of quantum filter diagonalization developed here, while the second of these variants lies closer to an extended version of the Kyriienko quantum inverse iteration method. Notably, in classical filter diagonalization approaches, the same final classical generalized eigenproblem arises as we encounter below. The key difference between classical and quantum filter diagonalization is that the Hamiltonian and metric matrix elements must be approximated by sparsity considerations or Monte Carlo integration in the classical approach, while we instead use a quantum circuit to efficiently evaluate the matrix elements in the quantum approach. It also worth pointing out that our QFD method was heavily inspired by Suzuki *et al*’s recent method for amplitude estimation without phase estimation,⁶⁹ in which it was shown that the PEA portions of a Grover-type amplitude estimation algorithm could be largely replaced by a larger set of quantum measurements performed over a variety of quantum circuits.

II. THEORY

A. Problem Statement

Consider a system of N qubits $\{A\}$. We are given a Hamiltonian operator in sparse Pauli form, e.g.,

$$\hat{H} \equiv \sum_A \mathcal{Z}_A \hat{Z}_A + \mathcal{X}_A \hat{X}_A \quad (1)$$

$$+ \sum_{A>B} \mathcal{Z} \mathcal{Z}_{AB} \hat{Z}_A \otimes \hat{Z}_B + \mathcal{Z} \mathcal{X}_{AB} \hat{Z}_A \otimes \hat{X}_B$$

$$+\mathcal{X}\mathcal{Z}_{AB}\hat{X}_A \otimes \hat{Z}_B + \mathcal{X}\mathcal{X}_{AB}\hat{X}_A \otimes \hat{X}_B + \dots$$

Here the ... indicates the possible presence of 3- and higher-body terms, but we do assume that the total number of terms scales polynomially in N . As written with only \hat{X} and \hat{Z} terms, the Hamiltonian is real symmetric - this is the case for all chemical Hamiltonians which we will encounter in the numerical test cases. However, all details of the QFD approach presented below would remain valid if the Hamiltonian was a more-general Hermitian operator with an imaginary antisymmetric component, e.g., \hat{Y} -type terms.

The objective is to determine an efficient recipe to conceptually prepare the lowest few eigenstates $\{|\Psi^\Theta\rangle\}$ and evaluate the corresponding eigenvalues $\{E^\Theta\}$,

$$\hat{H}|\Psi^\Theta\rangle = E^\Theta|\Psi^\Theta\rangle : \langle\Psi^\Theta|\Psi^{\Theta'}\rangle = \delta_{\Theta\Theta'} \quad (2)$$

And then to evaluate some low-order (transition) operator expectation values,

$$O^{\Theta\Theta'} \equiv \langle\Psi^\Theta|\hat{O}|\Psi^{\Theta'}\rangle \quad (3)$$

Where \hat{O} is also a low-order Hermitian Pauli operator. Note that the observables $\{E^\Theta\}$ and $\{O^{\Theta\Theta'}\}$ are all that we ultimately require - the eigenstates $\{|\Psi^\Theta\rangle\}$ are only conceptually useful, and never need to be explicitly represented classically.

B. Spectrum Normalization

In general, the Hamiltonian will present with an arbitrary spectral range $[E^{\min}, E^{\max}]$. To normalize the time propagation grid, we must determine a scaling parameter κ that brings the spectrum into the interval $[0, 1]$, modulo a constant phase factor,

$$\kappa \equiv E^+ - E^- \geq E^{\max} - E^{\min} + \Delta \quad (4)$$

Here Δ is a small overage to provide a gap between the lowest and highest eigenvalues upon mapping to the periodic domain $[0, 1]$. Efficient classical heuristic techniques such as the Gershgorin circle theorem can often be used to provide good estimates of E^- and E^+ .

C. QFD Ansatz

The variational ansatz for quantum filter diagonalization (QFD) is,

$$|\Psi^\Theta\rangle \equiv \sum_{\Xi k} C_{\Xi k}^\Theta e^{-i2\pi k \hat{H}/\kappa} |\Phi_\Xi\rangle \equiv \sum_{\Xi k} C_{\Xi k}^\Theta |\Gamma_{\Xi k}\rangle \quad (5)$$

Here $\{|\Phi_\Xi\rangle\}$ are a handful of easily-prepared guess states that are determined by classical preprocessing and that can be efficiently prepared by simple quantum circuits. The “time” index k covers integers from $-k_{\max}$ to $+k_{\max}$.

As $k_{\max} \rightarrow \infty$, the variational completeness of ansatz increases. The operator $\hat{U}_k \equiv e^{-i2\pi k \hat{H}/\kappa}$ is the time propagation operator, which provides a systematic way to extend the basis. We reserve the right to make minor definitional modifications to U_k later in this work, e.g., by approximating by a Trotterization procedure.

The only free parameters of the ansatz are the values of $C_{\Xi k}^\Theta$, which are determined through the variational Rayleigh-Ritz procedure by classically solving the subspace eigenvalue problem,

$$\begin{aligned} \sum_{\Xi' k'} \mathcal{H}_{\Xi k, \Xi' k'} C_{\Xi' k'}^\Theta &= \sum_{\Xi' k'} \mathcal{S}_{\Xi k, \Xi' k'} C_{\Xi' k'}^\Theta E^\Theta : \\ \sum_{\Xi k} \sum_{\Xi' k'} C_{\Xi k}^{*\Theta} \mathcal{S}_{\Xi k, \Xi' k'} C_{\Xi' k'}^\Theta &= \delta_{\Theta\Theta'} \end{aligned} \quad (6)$$

The all-important “quantum” matrix elements are the subspace Hamiltonian,

$$\begin{aligned} \mathcal{H}_{\Xi k, \Xi' k'} &\equiv \langle\Gamma_{\Xi k}|\hat{H}|\Gamma_{\Xi' k'}\rangle \\ &= \langle\Phi_\Xi|e^{+i2\pi k \hat{H}/\kappa} \hat{H} e^{-i2\pi k' \hat{H}/\kappa} |\Phi_{\Xi'}\rangle \end{aligned} \quad (7)$$

and the subspace metric,

$$\begin{aligned} \mathcal{S}_{\Xi k, \Xi' k'} &\equiv \langle\Gamma_{\Xi k}|\Gamma_{\Xi' k'}\rangle \\ &= \langle\Phi_\Xi|e^{+i2\pi k \hat{H}/\kappa} e^{-i2\pi k' \hat{H}/\kappa} |\Phi_{\Xi'}\rangle \end{aligned} \quad (8)$$

Techniques developed below will enable the efficient evaluation of these matrix elements in terms of extended swap test quantum circuits with a single ancilla qubit. The evaluation of these matrix elements is trivially parallelizable across multiple quantum circuit hardware instances. Note that the variational parameters are all determined monolithically *after* evaluation of all quantum circuit matrix elements. Moreover, the classical generalized eigenproblem encountered has been extensively studied in classical electronic structure methods,⁷⁰ and can be solved with a pair of calls to a standard eigenproblem solver such as LAPACK’s ZHEEV. A spectral cutoff in the eigenvalues of the metric matrix can be used to ameliorate poor condition encountered during determination of the inverse square root of the metric matrix, a procedure referred to in electronic structure methods as canonical orthogonalization.

D. Transition Properties

After the completion of the algorithm, transition property expectation values over another Hermitian operator \hat{O} in sparse Pauli form may be evaluated as,

$$\langle\Psi^\Theta|\hat{O}|\Psi^{\Theta'}\rangle = \sum_{\Xi k} \sum_{\Xi' k'} C_{\Xi k}^{*\Theta} \mathcal{O}_{\Xi k, \Xi' k'} C_{\Xi' k'}^{\Theta'} \quad (9)$$

where the quantum matrix elements of the property operator are,

$$\begin{aligned} \mathcal{O}_{\Xi k, \Xi' k'} &\equiv \langle \Gamma_{\Xi k} | \hat{O} | \Gamma_{\Xi' k'} \rangle \\ &= \langle \Phi_{\Xi} | e^{+i2\pi k \hat{H}/\kappa} \hat{O} e^{-i2\pi k' \hat{H}/\kappa} | \Phi_{\Xi'} \rangle \end{aligned} \quad (10)$$

E. General Quantum Matrix Elements

Consider the N -qubit quantum states,

$$|A\rangle \equiv \hat{V}|\Omega\rangle \quad (11)$$

$$|B\rangle \equiv \hat{W}|\Omega\rangle \quad (12)$$

Here, $|\Omega\rangle$ is an arbitrary reference state, and \hat{V} and \hat{W} are arbitrary unitary operators. For an arbitrary Hermitian operator \hat{O} , we wish to evaluate the transition expectation value (generally a complex scalar quantity),

$$\langle A | \hat{O} | B \rangle \equiv \langle \Omega | \hat{V}^\dagger \hat{O} \hat{W} | \Omega \rangle \quad (13)$$

This can be accomplished by the following $N + 1$ -qubit quantum circuit with a single ancilla qubit,

$$|\aleph\rangle \equiv \frac{1}{\sqrt{2}} \left[|0\rangle \otimes \hat{V}|\Omega\rangle + |1\rangle \otimes \hat{W}|\Omega\rangle \right] \quad (14)$$

It can be easily shown that,

$$\langle A | \hat{O} | B \rangle = \langle \aleph | \hat{X} \otimes \hat{O} | \aleph \rangle + i \langle \aleph | \hat{Y} \otimes \hat{O} | \aleph \rangle \quad (15)$$

I.e., the required transition matrix elements between different basis states over Hermitian Pauli operators can be statistically estimated by Pauli measurements of an extended swap test circuit with one ancilla qubit. Viewed another way, this circuit is a somewhat generalized one-ancilla phase estimation algorithm (PEA) circuit.

F. Specific Quantum Matrix Elements

If brevity of notation and code were of prime importance, we would define $|\Omega\rangle \equiv |0\rangle$ and absorb the definition of the reference state into the controlled unitaries \hat{V} and \hat{W} . However, this would be somewhat wasteful in requiring the ancilla to control both time propagation and state preparation circuit elements. Instead, we adopt the convention that $|\Omega\rangle$ is defined to be an appropriately selected reference state, and the controlled unitaries \hat{V} and \hat{W} perform only time propagation operations. For the diagonal blocks $\Xi = \Xi'$, this is particularly easy: we define $|\Omega\rangle \equiv |\Phi_{\Xi}\rangle$, $\hat{V} \equiv e^{-i2\pi k \hat{H}/\kappa}$ and $\hat{W} \equiv e^{-i2\pi k' \hat{H}/\kappa}$ to obtain $\mathcal{H}_{\Xi k, \Xi' k'}$ and $\mathcal{S}_{\Xi k, \Xi' k'}$. For the off-diagonal blocks $\Xi \neq \Xi'$, the \hat{V} and \hat{W} operators remain unchanged, but

the $|\Omega\rangle$ state is redefined as one of the ‘‘interfering reference states,’’ defined as,

$$|\Phi_{\Xi \Xi'}^{\pm, \text{Re}}\rangle \equiv \frac{1}{\sqrt{2}} [|\Phi_{\Xi}\rangle \pm |\Phi_{\Xi'}\rangle] \quad (16)$$

and,

$$|\Phi_{\Xi \Xi'}^{\pm, \text{Im}}\rangle \equiv \frac{1}{\sqrt{2}} [|\Phi_{\Xi}\rangle \pm i|\Phi_{\Xi'}\rangle] \quad (17)$$

E.g.,

$$\begin{aligned} 2\text{Re}(\mathcal{H}_{\Xi k, \Xi' k'}) &\equiv 2\text{Re}\left(\langle \Gamma_{\Xi k} | \hat{H} | \Gamma_{\Xi' k'} \rangle\right) \\ &= \langle \Phi_{\Xi \Xi'}^+, \text{Re} | e^{+i2\pi k \hat{H}/\kappa} \hat{H} e^{-i2\pi k' \hat{H}/\kappa} | \Phi_{\Xi \Xi'}^+, \text{Re} \rangle \\ &\quad - \langle \Phi_{\Xi \Xi'}^-, \text{Re} | e^{+i2\pi k \hat{H}/\kappa} \hat{H} e^{-i2\pi k' \hat{H}/\kappa} | \Phi_{\Xi \Xi'}^-, \text{Re} \rangle \end{aligned} \quad (18)$$

and,

$$\begin{aligned} -2\text{Im}(\mathcal{H}_{\Xi k, \Xi' k'}) &\equiv -2\text{Im}\left(\langle \Gamma_{\Xi k} | \hat{H} | \Gamma_{\Xi' k'} \rangle\right) \\ &= \langle \Phi_{\Xi \Xi'}^+, \text{Re} | e^{+i2\pi k \hat{H}/\kappa} \hat{H} e^{-i2\pi k' \hat{H}/\kappa} | \Phi_{\Xi \Xi'}^+, \text{Re} \rangle \\ &\quad - \langle \Phi_{\Xi \Xi'}^-, \text{Re} | e^{+i2\pi k \hat{H}/\kappa} \hat{H} e^{-i2\pi k' \hat{H}/\kappa} | \Phi_{\Xi \Xi'}^-, \text{Re} \rangle \end{aligned} \quad (19)$$

and similarly for $\mathcal{S}_{\Xi k, \Xi' k'}$. To complete the formal definition of the matrix elements, $\hat{O} \equiv \hat{H}$ for $\mathcal{H}_{\Xi k, \Xi' k'}$ and $\hat{O} \equiv \hat{I}$ for $\mathcal{S}_{\Xi k, \Xi' k'}$.

G. Trotterization (for Quantum Hamiltonian Diagonalization)

At this point, one might ask why we did not instantly exploit the property of time translational invariance in the evaluation of the Hamiltonian and metric quantum matrix elements. Explicitly, the elements of each Ξ, Ξ' subblock of these two matrices are Toeplitz as written, i.e., $\mathcal{H}_{\Xi k, \Xi' k'} = \mathcal{H}_{\Xi, \Xi'}^{k' - k}$. Unfortunately, for quantum Hamiltonians, we cannot *quite* evaluate such matrix elements in standard quantum circuit hardware. The reason for this is that the exponential over a direct sum of noncommuting Pauli operators must be approximated by a procedure such as Trotterization (also called Suzuki-Trotter splitting). Trotterization necessarily induces moderate errors relative to the desired exact time propagation operator. It is plausible that one could reduce these errors to a negligible level with sufficiently many Trotter steps, in which case the Trotterized quantum matrix elements would be statistically indistinguishable from the exact quantum matrix elements. In such a case, the translational invariance property could be exploited to reduce the number of required quantum matrix

elements to linear in k_{\max} . Unfortunately, this approach is likely to require too many Trotter steps to be tractable on NISQ-era hardware. Moreover, if any nontrivial errors arise from Trotterization, such an approach would lose the variational property, and the clean picture of a wavefunction ansatz would be lost. Instead, we have elected to inject the Trotterization into the definition of the basis functions,

$$|\Gamma_{\Xi k}\rangle \equiv e^{-i2\pi k\hat{H}/\kappa}|\Phi_{\Xi}\rangle \leftarrow \hat{U}_{\text{Trotter}}\left(2\pi k\hat{H}/\kappa\right)|\Phi_{\Xi}\rangle \quad (20)$$

This breaks the Toeplitz property of the quantum matrix elements (necessitating the evaluation of a quadratic number of matrix elements in k_{\max}), but retains the clear and numerically robust picture of a variational wavefunction ansatz. For instance, the exact solution is still obtained as $k_{\max} \rightarrow \infty$ with our approach, which is not obtained if the Trotterization is applied post facto within the Toeplitz quantum matrix elements. Moreover, we believe that the parallel evaluation of a quadratic number of low-depth quantum matrix elements is much more likely to be feasible on NISQ-era hardware than the evaluation of a linear number of high-depth quantum matrix elements.

H. Explicit QFD Procedure

The explicit steps of the QFD procedure are summarized as follows:

1. Classically compute the sparse Pauli matrix elements of the Hamiltonian and other desired observable operators, e.g., $\{\mathcal{Z}_A\}$ and similar in Equation 1.
2. Determine the spectral scaling parameter κ of Equation 4 by a classical preprocessing approach such as a heuristic estimate of the Gershgorin circle theorem.
3. Classically determine the characteristics of the guess states $\{|\Phi_{\Xi}\rangle\}$ and develop efficient quantum circuits to prepare these states (and linear combinations of pairs thereof). For quantum Hamiltonian diagonalization, a heuristic approximation like configuration interaction singles (CIS) might be used.
4. Use the extended swap test quantum circuits of Equation 14 and variants thereof described around Equation 16 to statistically estimate the matrix elements of the subspace Hamiltonian $\mathcal{H}_{\Xi k, \Xi' k'}$ of Equation 7 and the subspace metric $\mathcal{S}_{\Xi k, \Xi' k'}$ of Equation 8. Importantly, the Pauli expectation values involved in both operators should be computed from the same set of quantum circuit measurements, to maximize the propensity for error cancellation due to correlated sampling. Trotterization of the time-propagation operators should be included variationally as described in equation 20.
5. Classically solve the subspace generalized eigenvalue problem of Equation 6 to determine the QFD variational parameters $\{C_{\Xi k}^{\Theta}\}$ and the Ritz estimates of the eigenvalues $\{E^{\Theta}\}$.
6. Evaluate desired transition expectation values $\{O^{\Theta\Theta'}\}$ through the subspace expectation value formula of Equation 9. Importantly, the subspace operator matrix elements $\mathcal{O}_{\Xi k, \Xi' k'}$ of Equation 10 often can reuse the quantum circuit measurements performed to obtain the subspace Hamiltonian and metric matrices in in Step 4 above.

III. RESULTS AND DISCUSSION

A. Demonstration System

For a practical exploration of the QFD approach, we have considered an *ab initio* exciton model (AIEM) Hamiltonian^{71–73} for a linear stack of $N = 8$ truncated BChl-a chromophore units, stacked in an aligned geometry and then allowed to geometrically relax with $\omega\text{PBE}(\omega = 0.3)/6\text{-}31\text{G}^*\text{-D3}$. An *ab initio* exciton model was constructed for this system using a TDA-TD-DFT $\omega\text{PBE}(\omega = 0.3)/6\text{-}31\text{G}^*$ treatment^{74,75} of the monomers and unrelaxed nearest-neighbor dipole-dipole couplings. This system requires an 8-qubit representation, and has a real 2-local Pauli Hamiltonian. The system setup and Hamiltonian matrix elements are reported in the main text and supplemental material of our MC-VQE paper.⁴²

B. Spectral Normalization

A prerequisite for QFD is a heuristic approach to estimate the spectral range of \hat{H} and determine the bounding parameter κ . Figure 1 depicts the full eigenspectrum and Gershgorin circle theorem analysis for this system. The results are congruent with our overall observations of more-general sets of AIEM Hamiltonians: the spectral range generally grows linearly with N , and the edges of the spectrum have significantly lower density of states than the exponential crowding encountered in the middle of the spectrum. The Gershgorin disks are generally wholly overlapping, i.e., there are no topological gaps in the eigenspectrum. The Gershgorin disks for the first and last row of the Hamiltonian, corresponding to the all-ground-state $|00\dots\rangle$ configuration and all-excited-state $|11\dots\rangle$ configuration are heuristically found to provide the extremal Gershgorin circles in all cases we have encountered. This is not a rigorous result, but provides a good starting point for more-advanced classical approaches that will rigorously bound the spectrum in polynomial effort. Note that it is not generally possible to explicitly classically evaluate all of the Gershgorin disks, as the size of the diagonal of the Hamiltonian grows as 2^N . For today, we will use these heuristically extremal

Gershgorin disks to determine κ . We note that this actually provides a reasonably tight bound in practice: the true spectral range is generally overestimated by only 30 – 50% by the first/last Gershgorin disk estimate for all AIEM systems we have yet encountered.

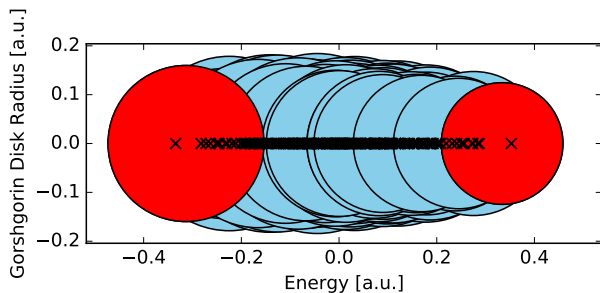


FIG. 1: Eigenspectrum and Gershgorin circle theorem analysis for $N = 8$ BChl-a AIEM Hamiltonian. The eigenvalues of \hat{H} are given by small x symbols on the x axis. The Gershgorin disks are presented as blue circles. The Gershgorin disks for the first and last row of the Hamiltonian, corresponding to the all-ground-state $|00\dots\rangle$ configuration and all-excited-state $|11\dots\rangle$ configuration, are presented as red disks.

C. Exact Time Propagation

Figure 2 depicts a simulated absorption spectrum for the $N = 8$ linear stack BChl-a test case. Excitation energies $\Delta E^\Theta \equiv E^\Theta - E^0$ and oscillator strengths $O^{0\Theta} \equiv (2/3)\Delta E^\Theta \langle |\Psi_0| \hat{\mu} | \Psi_\Theta \rangle|^2$ are computed for each method, and compared to full configuration interaction (FCI). Configuration interaction singles (CIS) including the reference configuration $|00\dots\rangle$ and all singly-excited configurations $|10\dots\rangle, |01\dots\rangle, \dots$ are used to provide QFD guess states $\{|\Phi_\Xi\rangle\}$. In this example, 9 states are targeted, starting from 9 guess states. This example uses an exact representation of the time propagation operator $\hat{U}_k \equiv e^{-i2\pi k \hat{H}/\kappa}$ representing an ideal infinite-order Trotter expansion of the time propagation circuit. The matrix elements $\mathcal{H}_{\Xi k, \Xi' k'}$ and $\mathcal{S}_{\Xi k, \Xi' k'}$ are obtained by contraction of the relevant statevectors to model infinite statistical sampling of the involved Pauli operators. This test probes the intrinsic limits of the QFD ansatz. The data indicates that the QFD series converges rapidly for this test case - even using a single k point, i.e., $k_{\max} = 1$, the improvement over the CIS guess is roughly one order of magnitude for all states and for both excitation energies and oscillator strengths. Moving to $k_{\max} = 2$, another order of magnitude improvement is obtained in both properties, and the resultant spectrum is visually indistinguishable from the reference full configuration interaction (FCI) spectrum. Moving to $k_{\max} = 3$, additional improvement is obtained, though the relative gains are somewhat smaller than in the first two increments.

By $k_{\max} = 3$, the errors in excitation energies are all at or below 10^{-3} eV, while the errors in oscillator strengths are all at or below 10^{-2} - essentially quantitative agreement. It is worth noting that the errors in excitation energies and especially in oscillator strengths are generally somewhat smaller and converge somewhat faster for lower-lying states.

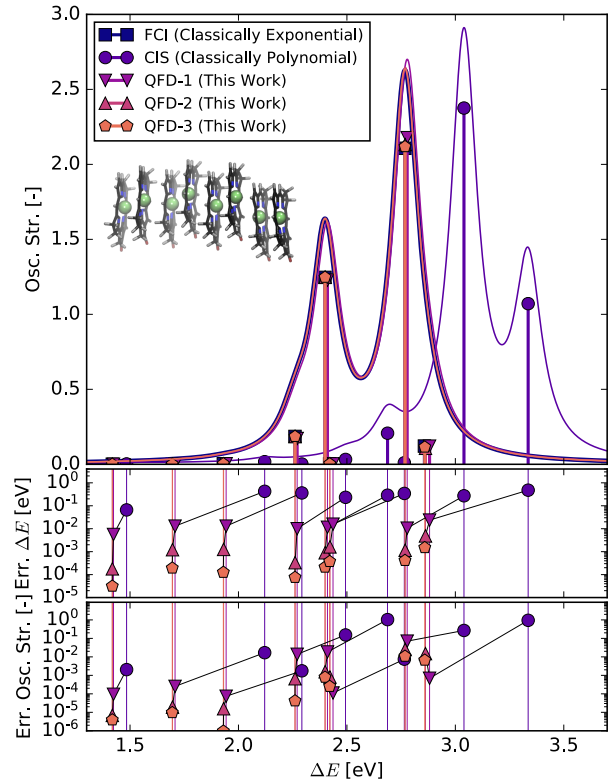


FIG. 2: Test of simulated QFD with exact representation of the time propagation operators vs. full configuration interaction (FCI) and configuration interaction singles (CIS). The notation QFD- k_{\max} means that the QFD time grid is truncated at k_{\max} , e.g., QFD-1 has $k_{\max} = 1$ and thus $k \in [-1, 0, +1]$. Top - Simulated absorption spectrum of $N = 8$ linear stack BChl-a test case (geometry depicted in inset), computed from the excitation energies and oscillator strengths of the lowest 8 electronic transitions, depicted as vertical sticks. The envelope of the absorption spectrum is sketched by broadening the contribution from each transition with a Lorentzian with width of $\delta = 0.15$ eV. Middle - errors in excitation energies. Bottom - errors in oscillator strengths. Middle and bottom - thin lines are a guide for the eye.

D. Trotterized Time Propagation (Variational)

Figure 3 depicts the equivalent of Figure 2, but with a physically realizable Trotter expansion of the time propagation operators. Here a single first-order Trotter step is applied for each unit of k (e.g., 2 Trotter steps for $k = 2$).

The first-order Trotter step is of the form,

$$e^{-i2\pi k \hat{H} / \kappa} \approx e^{-i2\pi k \hat{H}_{XX\dots} / \kappa} e^{-i2\pi k \hat{H}_{XZ\dots} / \kappa} \\ \times e^{-i2\pi k \hat{H}_{ZZ\dots} / \kappa} e^{-i2\pi k \hat{H}_{ZX\dots} / \kappa} \quad (21)$$

The \hat{X}_A one-body terms are grouped with $\hat{H}_{XX\dots}$ and the \hat{Z}_A one-body terms are grouped with $\hat{H}_{ZZ\dots}$. Comparing the data between Figures 3 and 2, it is apparent that even the remarkably coarse Trotter expansion employed here only marginally degrades the accuracy of the QFD ansatz. QFD-1 with Trotterization produces a more qualitatively divergent absorption spectrum than with exact time propagation, but the Trotterized QFD-2 is essentially quantitatively converged. Considering the lower panels of the figures, the Trotterized errors and convergence rates are marginally slower than with ideal time propagation. Overall, this is somewhat remarkable - the coarseness of the Trotterization employed here means that the Trotterized vs. exact time propagation operators differ significantly, but the QFD errors stemming from Trotterization at a given k_{\max} are generally of the same order of magnitude as changing from the previous k_{\max} to the next. We attribute this tolerance of coarse Trotterization to the use of a variational QFD ansatz: The Trotterized QFD basis states are significantly different than the exact basis states, but the coefficients are separately variationally optimized for each case, leading to only marginal accuracy degradation with coarse Trotterization.

A non-variational form of Trotterization was also implemented, and found to give exceedingly large errors even with small Trotter timesteps. This indicates that the variational property of the QFD ansatz is critical to providing an accurate representation, as expected. More details are provided in Appendix A below.

IV. SUMMARY AND OUTLOOK

We have discussed a quantum filter diagonalization method (QFD) with a set of time-propagated guess states forming a variational basis for the approximate Rayleigh-Ritz diagonalization of sparse Pauli operators. The variational parameters of the method are determined through a one-shot classical solution of a generalized eigenproblem in a small subspace of the full Hilbert space, while observations of quantum circuits are used to compute the subspace matrix elements needed as the input of this generalized eigenproblem. The method converges monotonically toward the exact eigenpairs with a single discrete k_{\max} parameter determining the completeness of the time grid expansion, and has been shown to be naturally applicable to the computation of ground- and excited-state eigenvalues and transition properties. Ideal classical simulations of the method have been shown to give accurate results for an example 8-qubit study involving the computation of the emphab initio exciton model (AIEM) absorption spectrum of a stack of 8 BChl-a chromophores.

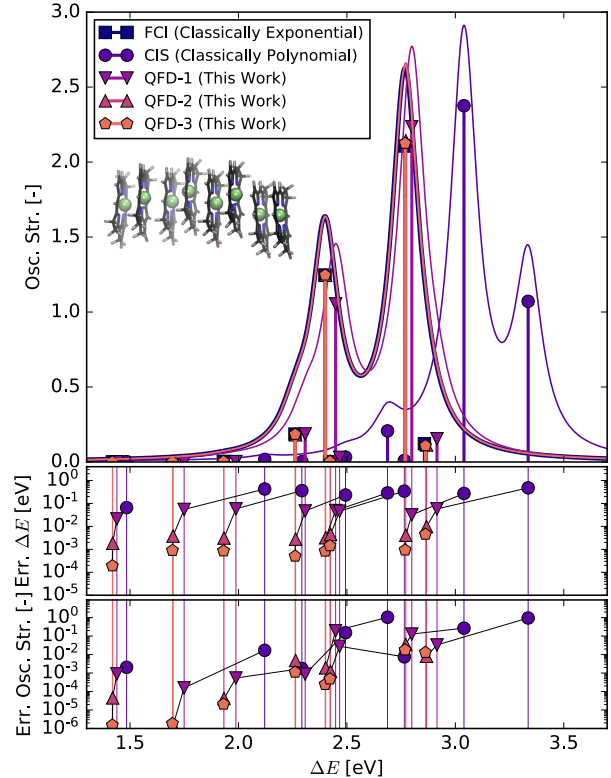


FIG. 3: Test of simulated QFD with Trotterized representation of the time propagation operators vs. full configuration interaction (FCI) and configuration interaction singles (CIS). One Trotter step per k point is used. The notation QFD- k_{\max} means that the QFD time grid is truncated at k_{\max} , e.g., QFD-1 has $k_{\max} = 1$ and thus $k \in [-1, 0, +1]$. Top - Simulated absorption spectrum of $N = 8$ linear stack BChl-a test case (geometry depicted in inset), computed from the excitation energies and oscillator strengths of the lowest 8 electronic transitions, depicted as vertical sticks. The envelope of the absorption spectrum is sketched by broadening the contribution from each transition with a Lorentzian with width of $\delta = 0.15$ eV. Middle - errors in excitation energies. Bottom - errors in oscillator strengths. Middle and bottom - thin lines are a guide for the eye.

High accuracy is obtained for both excitation energies and oscillator strengths with only a handful of k points and with remarkably coarse Trotter expansions of the time propagation operators. The rather minor degradation of performance upon Trotterization is attributed to the variational property of the Trotterized QFD basis functions - a conceptual experiment involving a nonvariational variant of QFD where Trotterization is performed after formal algebraic simplifications of the quantum matrix elements yielded vanishingly accurate results.

The QFD method occupies an interesting place relative to other quantum algorithms for eigendecomposition. When compared to VQE, it appears that the QFD controlled swap test circuits might be only marginally

longer than VQE entangler circuits, while the straightforward QFD ansatz may remove some of the conceptual difficulties with designing an optimizing heuristic VQE entangler circuits. Relative to PEA, QFD uses many more evaluations of short quantum circuits to build toward a complete picture of the relevant subblock of the partially diagonalized Hamiltonian. Therefore, QFD is potentially much more tractable with NISQ-era quantum hardware than QFD, but will necessarily rely on spectral structure such as nonvanishing average gaps in the relevant energy windows to produce accurate results with short time expansions. Another interesting distinction between PEA and QFD is that the former extracts the eigenvalues of a unitary operator while the latter extracts the eigenvalues of a Hamiltonian operator. In an ideal world, these would contain equivalent information which would be extractable through knowledge of the exponential map. However, in a Trotterized environment, QFD has the intriguing possibility that the quality of the Hamiltonian eigenvalue estimate does not appear to be limited by the quality of the Trotterization.

Relative to other recent time-grid quantum algorithms, QFD appears to occupy a somewhat different portion of the algorithmic landscape in the emergence, explicit computation, and subsequent diagonalization of a variational subspace eigenproblem. This avoids the requirement to parametrize an explicit filter function with detailed knowledge of the approximate eigenspectrum, e.g., there is no need to define a spectral cutoff in the QFD method. To some extent, the method resembles the Davidson approach of classical electronic structure theory where one is able to compute and store full matrix-vector products, and iteratively diagonalizes a subspace Hamiltonian. However, the Davidson procedure has an additional advantage over QFD in that the Ritz estimates for the eigenpairs from each stage of the decomposition are used to “boost” the convergence by preconditioning. This was recently demonstrated in the quantum inverse iteration method for ground-state eigendecomposition, where the action of $(\hat{H} - \lambda)^{-\alpha}$ on a guess state was expanded as a time grid, and used to amplify the component of the eigenpair closest to λ in the guess state. It would be very interesting to consider merging some of the boosting ideas from quantum inverse iteration with the subspace diagonalization of quantum filter diagonalization to obtain a method even closer in spirit to the Davidson approach. One might also consider other approaches where a classical solution of a subspace eigenproblem over quantum-enabled basis states is invoked. For instance, one could imagine constructing a basis of state-specific VQE states $|\Gamma_{\Xi}\rangle \equiv \hat{U}_{\Xi}|\Phi_{\Xi}\rangle$, diagonalizing the subspace eigenproblem to determine the mixing of the basis states, and then iteratively optimizing the VQE parameters to minimize the sum of the resultant eigenvalues. Overall, all of these approaches are moving toward an environment in which the target eigenvector is approximated by

a classical weighted sum of statevectors prepared by different quantum circuits.

It will be useful to explore the characteristics of QFD in practice. One challenge will be the design of physical quantum circuits performing the one-ancilla controlled swap tests needed for the subspace matrix elements. Another potential challenge is the accurate solution of the subspace eigenproblem in the presence of statistical or device noise channels. Here, it seems plausible that correlations in the noise between the subspace Hamiltonian and subspace metric matrices (which may be evaluated simultaneously with the same set of Pauli measurements), may help mitigate this potential issue. Overall, it will be interesting to continue pushing down the general track of time grid methods: it is certainly possible that the no free lunch theorem somehow still holds here, but the glimmering alternative is a series of methods with wide near-term applicability that are much more tractable than full phase estimation.

Acknowledgements: RMP thanks Prof. Todd J. Martínez for many interesting discussions on classical filter diagonalization approaches and related methods. RMP and PLM acknowledge Mr. Joseph T. Iosue and Prof. Wim van Dam for useful discussions on the extended swap test. RMP and PLM own stock/options in QC Ware Corporation.

Appendix A: Trotterized Time Propagation (Nonvariational)

To probe the importance of the variational property in QFD, we have implemented a nonvariational form of QFD, where formal time-translational invariance property with exact time propagation is first used to write the QFD subspace Hamiltonian matrix elements (and similarly the QFD subspace metric matrix elements) as,

$$\mathcal{H}_{\Xi k, \Xi' k'} = \langle \Phi_{\Xi} | \hat{H} e^{-i2\pi(k' - k)\hat{H}/\kappa} | \Phi_{\Xi'} \rangle \quad (\text{A1})$$

which reduces the number of formally unique matrix elements from $(2k_{\max} + 1)^2$ to $4k_{\max} + 1$. The Trotterization procedure is then applied *after* the formal manipulations of the matrix elements, resulting in a physically realizable but nonvariational QFD method.

The performance of this method is drastically degraded relative to variational QFD, to the point that nonvariational errors larger than the excitation energies are encountered even with very small Trotter timesteps. In fact, we were only able to achieve accurate results with the nonvariational QFD approach for $k_{\max} = 1$ with overwhelmingly long Trotterizations with 100-1000 steps. This highlights the expected importance of the variational property within the preferred QFD method developed above.

- * Electronic address: rob.parrish@qcware.com
- ¹ P. Hohenberg and W. Kohn, Phys. Rev. **136**, B864 (1964).
 - ² W. Kohn and L. J. Sham, Phys. Rev. **140**, A1133 (1965).
 - ³ E. Runge and E. K. Gross, Phys. Rev. Lett. **52**, 997 (1984).
 - ⁴ W. Koch and M. C. Holthausen, *A Chemist's Guide to Density Functional Theory*, Wiley-VCH, New York, 2001.
 - ⁵ J. Cížek, J. Chem. Phys. **45**, 4256 (1966).
 - ⁶ G. D. Purvis and R. J. Bartlett, J. Chem. Phys. **76**, 1910 (1982).
 - ⁷ T. D. Crawford and H. F. Schaefer, *An Introduction to Coupled Cluster Theory for Computational Chemists*, pages 33–136, Wiley-Blackwell, 2007.
 - ⁸ I. Shavitt and R. Bartlett, *Many-Body Methods in Chemistry and Physics: MBPT and Coupled-Cluster Theory*, Cambridge Molecular Science, Cambridge University Press, 2009.
 - ⁹ J. E. Deustua, J. Shen, and P. Piecuch, Phys. Rev. Lett. **119**, 223003 (2017).
 - ¹⁰ J. E. Deustua, I. Magoulas, J. Shen, and P. Piecuch, J. Chem. Phys. **149**, 151101 (2018).
 - ¹¹ C. F. Bender and E. R. Davidson, Phys. Rev. **183**, 23 (1969).
 - ¹² B. Huron, J. Malrieu, and P. Rancurel, J. Chem. Phys. **58**, 5745 (1973).
 - ¹³ G. H. Booth, A. J. Thom, and A. Alavi, J. Chem. Phys. **131**, 054106 (2009).
 - ¹⁴ D. Cleland, G. Booth, and A. Alavi, J. Chem. Phys. **132**, 041103 (2010).
 - ¹⁵ A. A. Holmes, N. M. Tubman, and C. Umrigar, J. Chem. Theory Comput. **12**, 3674 (2016).
 - ¹⁶ J. B. Schriber and F. A. Evangelista, J. Chem. Phys. **144**, 161106 (2016).
 - ¹⁷ J. B. Schriber and F. A. Evangelista, J. Chem. Theory Comput. **13**, 5354 (2017).
 - ¹⁸ S. R. White, Phys. Rev. Lett. **69**, 2863 (1992).
 - ¹⁹ G. K.-L. Chan and S. Sharma, Ann. Rev. Phys. Chem. **62**, 465 (2011).
 - ²⁰ A. Y. Kitaev, arXiv preprint quant-ph/9511026 (1995).
 - ²¹ D. S. Abrams and S. Lloyd, Phys. Rev. Lett. **79**, 2586 (1997).
 - ²² R. Cleve, A. Ekert, C. Macchiavello, and M. Mosca, Proceedings of the Royal Society of London. Series A: Mathematical, Physical and Engineering Sciences **454**, 339 (1998).
 - ²³ D. S. Abrams and S. Lloyd, Phys. Rev. Lett. **83**, 5162 (1999).
 - ²⁴ A. Aspuru-Guzik, A. D. Dutoi, P. J. Love, and M. Head-Gordon, Science **309**, 1704 (2005).
 - ²⁵ B. P. Lanyon et al., Nat. Chem. **2**, 106 (2010).
 - ²⁶ D. Wecker, B. Bauer, B. K. Clark, M. B. Hastings, and M. Troyer, Phys. Rev. A **90**, 022305 (2014).
 - ²⁷ N. M. Tubman et al., arXiv preprint arXiv:1809.05523 (2018).
 - ²⁸ J. Preskill, Quantum **2**, 79 (2018).
 - ²⁹ A. Peruzzo et al., Nat. Comm. **5**, 4213 (2014).
 - ³⁰ J. R. McClean, J. Romero, R. Babbush, and A. Aspuru-Guzik, New J. Phys. **18**, 023023 (2016).
 - ³¹ P. O'Malley et al., Phys. Rev. X **6**, 031007 (2016).
 - ³² A. Kandala et al., Nature **549**, 242 (2017).
 - ³³ J. R. McClean et al., arXiv preprint arXiv:1710.07629 (2017).
 - ³⁴ J. Romero et al., Quant. Sci. Tech. **4**, 014008 (2018).
 - ³⁵ Y. Nam et al., arXiv preprint arXiv:1902.10171 (2019).
 - ³⁶ Q. Gao et al., arXiv e-prints, arXiv:1906.10675 (2019).
 - ³⁷ J. R. McClean, M. E. Kimchi-Schwartz, J. Carter, and W. A. de Jong, Phys. Rev. A **95**, 042308 (2017).
 - ³⁸ O. Higgott, D. Wang, and S. Brierley, arXiv preprint arXiv:1805.08138 (2018).
 - ³⁹ J. Lee, W. J. Huggins, M. Head-Gordon, and K. B. Whaley, J. Chem. Theory Comput. (2018).
 - ⁴⁰ J. I. Colless et al., Phys. Rev. X **8**, 011021 (2018).
 - ⁴¹ K. M. Nakanishi, K. Mitarai, and K. Fujii, arXiv preprint arXiv:1810.09434 (2018).
 - ⁴² R. M. Parrish, E. G. Hohenstein, P. L. McMahon, and T. J. Martínez, Phys. Rev. Lett. **122**, 230401 (2019).
 - ⁴³ T. E. O'Brien et al., arXiv e-prints, arXiv:1905.03742 (2019).
 - ⁴⁴ K. Mitarai, Y. O. Nakagawa, and W. Mizukami, arXiv e-prints, arXiv:1905.04054 (2019).
 - ⁴⁵ R. M. Parrish, E. G. Hohenstein, P. L. McMahon, and T. J. Martínez, arXiv preprint arXiv:1906.08728 (2019).
 - ⁴⁶ E. Farhi, J. Goldstone, and S. Gutmann, arXiv preprint arXiv:1411.4028 (2014).
 - ⁴⁷ A. Lucas, Frontiers in Physics **2**, 5 (2014).
 - ⁴⁸ E. Farhi, J. Goldstone, S. Gutmann, and H. Neven, arXiv preprint arXiv:1703.06199 (2017).
 - ⁴⁹ J. Otterbach et al., arXiv preprint arXiv:1712.05771 (2017).
 - ⁵⁰ N. Moll et al., Quantum Science and Technology **3**, 030503 (2018).
 - ⁵¹ G. E. Crooks, arXiv preprint arXiv:1811.08419 (2018).
 - ⁵² L. Zhou, S.-T. Wang, S. Choi, H. Pichler, and M. D. Lukin, arXiv preprint arXiv:1812.01041 (2018).
 - ⁵³ F. G. Brandao, M. Broughton, E. Farhi, S. Gutmann, and H. Neven, arXiv preprint arXiv:1812.04170 (2018).
 - ⁵⁴ F. Glover and G. Kochenberger, arXiv preprint arXiv:1811.11538 (2018).
 - ⁵⁵ S. Hadfield et al., Algorithms **12**, 34 (2019).
 - ⁵⁶ A. Gilyén, S. Arunachalam, and N. Wiebe, Optimizing quantum optimization algorithms via faster quantum gradient computation, in *Proceedings of the Thirtieth Annual ACM-SIAM Symposium on Discrete Algorithms*, pages 1425–1444, SIAM, 2019.
 - ⁵⁷ G. Nannicini, Physical Review E **99**, 013304 (2019).
 - ⁵⁸ J. R. McClean, S. Boixo, V. N. Smelyanskiy, R. Babbush, and H. Neven, Nature communications **9**, 4812 (2018).
 - ⁵⁹ R. Somma, G. Ortiz, J. E. Gubernatis, E. Knill, and R. Laflamme, Physical Review A **65**, 042323 (2002).
 - ⁶⁰ T. E. O'Brien, B. Tarasinski, and B. Terhal, New Journal of Physics (2019).
 - ⁶¹ O. Kyriienko, arXiv preprint arXiv:1901.09988 (2019).
 - ⁶² R. D. Somma, arXiv e-prints, arXiv:1907.11748 (2019).
 - ⁶³ D. Neuhauser, The Journal of Chemical Physics **93**, 2611 (1990).
 - ⁶⁴ D. Neuhauser, J. Chem. Phys. **100**, 5076 (1994).
 - ⁶⁵ T. P. Grozdanov, V. A. Mandelshtam, and H. S. Taylor, J. Chem. Phys. **103**, 7990 (1995).
 - ⁶⁶ V. A. Mandelshtam and H. S. Taylor, J. Chem. Phys. **102**, 7390 (1995).
 - ⁶⁷ M. R. Wall and D. Neuhauser, J. Chem. Phys. **102**, 8011 (1995).
 - ⁶⁸ V. A. Mandelshtam and H. S. Taylor, J. Chem. Phys. **106**,

- 5085 (1997).
- ⁶⁹ Y. Suzuki et al., arXiv e-prints , arXiv:1904.10246 (2019).
- ⁷⁰ A. Szabo and N. S. Ostlund, *Modern quantum chemistry: introduction to advanced electronic structure theory*, Courier Corporation, 2012.
- ⁷¹ A. Sisto, D. R. Glowacki, and T. J. Martinez, *Acc. Chem. Res.* **47**, 2857 (2014).
- ⁷² A. Sisto et al., *Phys. Chem. Chem. Phys.* **19**, 14924 (2017).
- ⁷³ X. Li, R. M. Parrish, F. Liu, S. I. Kokkila Schumacher, and T. J. Martínez, *J. Chem. Theory Comput.* **13**, 3493 (2017).
- ⁷⁴ Y. Tawada, T. Tsuneda, S. Yanagisawa, T. Yanai, and K. Hirao, *J. Chem. Phys.* **120**, 8425 (2004).
- ⁷⁵ O. A. Vydrov and G. E. Scuseria, *J. Chem. Phys.* **125**, 234109 (2006).